



Analysis and prediction model of ferroptosis related genes in breast cancer

Lingli Wang, Yi Chen, Jianjie Zhao, Donglin Luo, Wuguo Tian

Department of Breast and Thyroid Surgery, Daping Hospital, Army Military Medical University, Chongqing, China

Contributions: (I) Conception and design: L Wang, W Tian; (II) Administrative support: D Luo; (III) Provision of study materials or patients: Y Chen, J Zhao; (IV) Collection and assembly of data: L Wang, W Tian; (V) Data analysis and interpretation: J Zhao, Y Chen; (VI) Manuscript writing: All authors; (VII) Final approval of manuscript: All authors.

Correspondence to: Wuguo Tian. Department of Breast and Thyroid Surgery, Daping Hospital, Army Military Medical University, Chongqing 400042, China. Email: tianwuguogood@126.com.

Background: The prognosis of patients with breast cancer (BRCA) is difficult to predict because of the high degree of heterogeneity and complex etiological factors. Ferroptosis, an iron-dependent, new form of cell death, plays an important role in regulation of tumor growth and progression. The aim of this study was to clarify the predictive value of ferroptosis-related genes in the overall survival of patients with BRCA.

Methods: The messenger RNA expression profile and clinical information of patients with BRCA were collected from The Cancer Genome Atlas (TCGA) database. The differences between BRCA and adjacent normal tissues were analyzed, and candidates with differentially expressed ferroptosis-related genes were identified. Through Cox and LASSO analyses, the prognostic genetic characteristics of ferroptosis-related genes were established. Lastly, according to the median risk score, the patients were divided into high-risk and low-risk groups, a nomogram was constructed, and the prediction accuracy was tested.

Results: It was determined that the four ferroptosis related genes had a significant difference in survival in BRCA ($P < 0.05$); a prognostic model was constructed based on the four ferroptosis related genes, and the overall survival of patients in the high-risk group was significantly worse ($P < 0.05$). The four-gene nomogram can quantify the contribution of each index to survival, and the calibration chart shows high prediction accuracy.

Conclusions: This study constructed four ferroptosis related gene characteristics and nomogram, which can effectively predict the prognosis of BRCA patients and provide new insights for future anti-cancer treatments based on ferroptosis targets.

Keywords: Ferroptosis; gene prognostic characteristics; nomogram; breast cancer (BRCA)

Submitted Dec 01, 2021. Accepted for publication May 26, 2022.

doi: 10.21037/tcr-21-2686

View this article at: <https://dx.doi.org/10.21037/tcr-21-2686>

Introduction

Breast cancer (BRCA) is the main cause of cancer-related death in women. The latest data show that approximately 2.1 million new occurrences of BRCA were diagnosed in 2018, accounting for 25% of all female cancers (1). In China, BRCA ranks first in the incidence of malignant tumors in females; its mortality rate ranks fifth and has been increasing in recent years (2). As treatment methods continue to improve, molecular classification has changed

the pattern of treatment. According to tumor stage, grade, human epidermal growth factor receptor 2, hormone receptor status, and tumor proliferation index, molecular classification provides a reference for clinical treatment selection and prognosis evaluation (3,4). BRCA is a highly heterogeneous tumor; different molecular types have different prognosis, and there are also differences in the same molecular type (5). Therefore, it is important to explore new treatment directions to improve survival prediction

performance.

Selective induction of cancer cell death is one of the most effective treatment methods for tumors. One such method is ferroptosis, which is closely related to various diseases, especially cancer, and plays a key role in all aspects of cancer biology and drug resistance (6). Ferroptosis is a new type of non-apoptosis regulated cell death that inhibits or promotes tumor progression by releasing a variety of signaling molecules in the tumor microenvironment (7). A study has confirmed that p53 promotes tumor cell ferroptosis through regulation and reduces the probability of distant tumor metastasis (8). Ferroptosis also affects tumor resistance and cancer immunotherapy (9,10). Recently, one study has shown that triple-negative BRCA is more sensitive to ferroptosis than hormone receptor-positive BRCA, which suggests that ferroptosis could be an effective treatment strategy for triple-negative BRCA (11). However, there remains a need for more extensive research on the application of ferroptosis towards the treatment of BRCA. Therefore, this study aimed to explore the mechanism and biological behavior of ferroptosis by obtaining information on BRCA patients from The Cancer Genome Atlas (TCGA) database. We also sought to identify potential treatment strategies for BRCA. We present the following article in accordance with the STREGA reporting checklist (available at <https://tcra.meagroups.com/article/view/10.21037/tcr-21-2686/rc>).

Methods

Data collection

RNA-sequencing expression (level 3) profiles and corresponding clinical information for BRCA were downloaded from TCGA dataset (<https://portal.gdc.cancer.gov/legacy-archive/search/f>). A total of 113 paracancerous samples were collected from TCGA database and 54 samples were collected from non-diseased tissue sites in GTEx.

Bioinformatics analysis

We used R (v4.0.3) software packages “ggplot2” and “pheatmap” to plot 25 ferroptosis-related genes (*CDKN1A*, *HSPA5*, *EMC2*, *SLC7A11*, *NFE2L2*, *MT1G*, *HSPB1*, *GPX4*, *FANCD2*, *CISD1*, *FDFT1*, *SLC1A5*, *SAT1*, *TFRC*, *RPL8*, *NCOA4*, *LPCAT3*, *GLS2*, *DPP4*, *CS*, *CARS1*, *ATP5MC3*, *ALOX15*, *ACSL4*, and *ATL1*). This was done to create heat maps of differential expression in BRCA and

normal control samples and to conduct correlation analysis. Ferroptosis-related genes were derived from a systematic analysis of the abnormalities and functions of ferroptosis in cancer by Liu *et al.* (12).

Survival analysis

Kaplan-Meier (KM) curves were drawn using R software packages “survival” and “survminer”. Log-rank was used to test the KM survival analysis and to compare the survival difference of the above-mentioned ferroptosis-related genes in BRCA; the P value ($P < 0.05$) was considered statistically significant.

Prognostic model establishment

A LASSO regression algorithm was used to select the characteristics of BRCA ferroptosis-related genes using 10-fold cross-validation; log-rank was used to test the KM survival analysis and compare the survival differences between the two groups of high and low wind directions. Lastly, time receiver operating characteristic (ROC) analysis was conducted to compare the accuracy of the predicted sex and risk scores for five genes.

Establishment of a nomogram

Uni-factor and multi-factor Cox regression analysis was performed using forest plots through the “forestplot” R package to display the P value, hazard ratio, and 95% confidence interval of each variable. Based on the results of the multivariate Cox proportional hazard analysis, the R software package “rms” was used to establish a nomogram to predict 3–5 years of disease-specific survival.

Statistical analysis

Bioinformatics analyses of databases were described in detail in the above method. The two-sided Student’s *t*-test was used to compare the differences between groups. KM analysis was performed via KM plotter. All assays were performed using R (4.0.3). $P < 0.05$ was considered statistically significant.

Ethical statement

The study was conducted in accordance with the Declaration of Helsinki (as revised in 2013). TCGA data

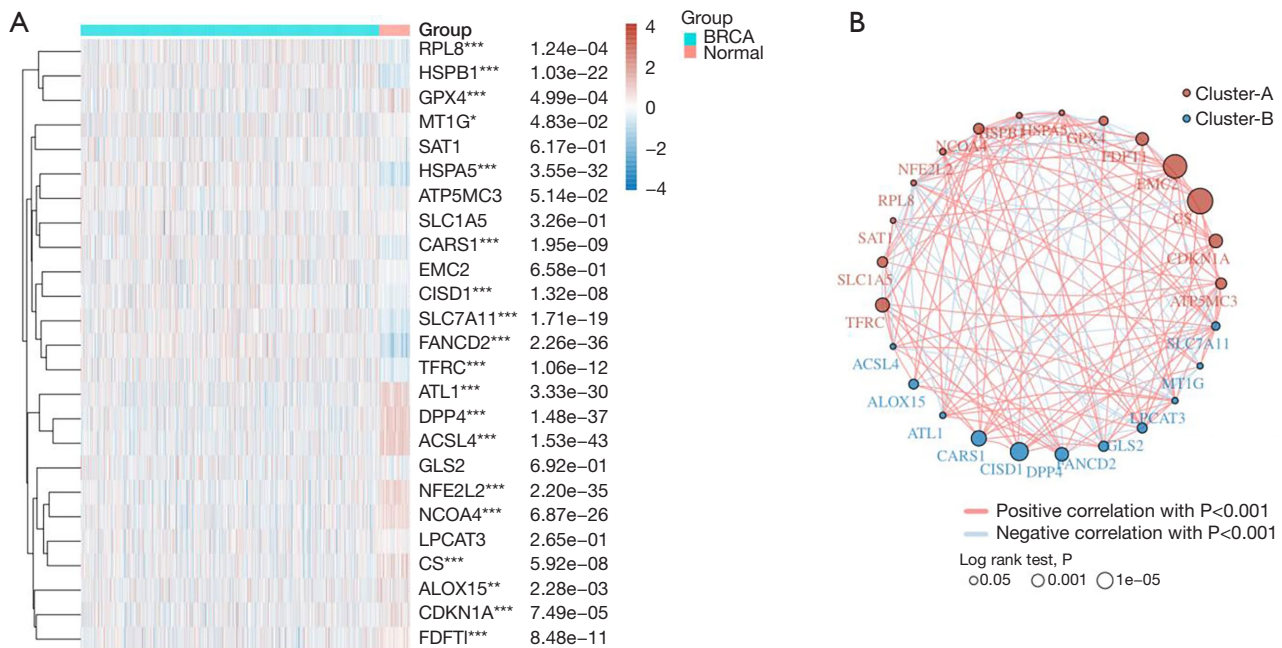


Figure 1 Heat map and correlation of breast cancer ferroptosis-related gene expression. (A) Different colors represent expression trends of ferroptosis-related genes in different samples. *, $P < 0.05$; **, $P < 0.01$; ***, $P < 0.001$; asterisks represent the degree of importance. (B) Circles represent ferroptosis-related genes; the larger the circle, the smaller the P value. The line represents the relationship between genes, where red represents a positive correlation, blue represents a negative correlation, and the line thickness represents how high or low the correlation is between the two genes. BRCA, breast cancer.

disclosure was available for this study without the approval of the ethics committee.

Results

Expression of ferroptosis-related genes in BRCA

Through the analysis of 25 ferroptosis-related genes (Table S1), 19 ferroptosis-related genes (*CDKN1A*, *HSPA5*, *SLC7A11*, *NFE2L2*, *MT1G*, *HSPB1*, *GPX4*, *FANCD2*, *CISD1*, *FDFT1*, *TFRC*, *RPL8*, *NCOA4*, *DPP4*, *CS*, *CARS1*, *ALOX15*, *ACSL4*, and *ATL1*) showed differences in tumors with BRCA compared to those in normal tissues (Figure 1A). The genes related to ferroptosis in BRCA are closely related. The most significant positive correlations were between *EMC2* and *CS*, and the most significant negative correlations were between *CISD1* and *CARS1* (Figure 1B).

Survival analysis and prognostic model establishment

Survival analysis of the differentially expressed genes revealed that the five ferroptosis-related genes, *CISD1*,

ALOX15, *CS*, *CARS1*, and *EMC2*, showed significant differences in survival in BRCA ($P < 0.05$); there was no significant survival difference in the other ferroptosis-related genes ($P < 0.05$; Figure 2). According to the expression profiles of the 19 ferroptosis-related genes obtained from the previous analysis, a prognosis model was constructed using LASSO Cox regression analysis. After regression analysis, the best four genes and their corresponding correlation coefficients were obtained.

The risk score was calculated as follows: risk score = $(0.361) \times CISD1 + (0.176) \times ALOX15 + (0.2704) \times CARS1 + (0.1208) \times SLC7A11$. According to the median risk score, patients were divided into a high-risk group (548 cases) and a low-risk group (548 cases; Figure 3A). The BRCA survival rate of the high-risk group was significantly higher than that of the low-risk group (Figure 3B). The KM survival analysis curve showed that the survival rate of the low-risk group was significantly higher than that of the high-risk group ($P < 0.001$; Figure 3C). The ROC curve was used to evaluate the predictive performance of the prognostic model. The area under the ROC curve was 0.641 at 3 years, 0.631 at 5 years, and 0.609 at 7 years (Figure 3D).

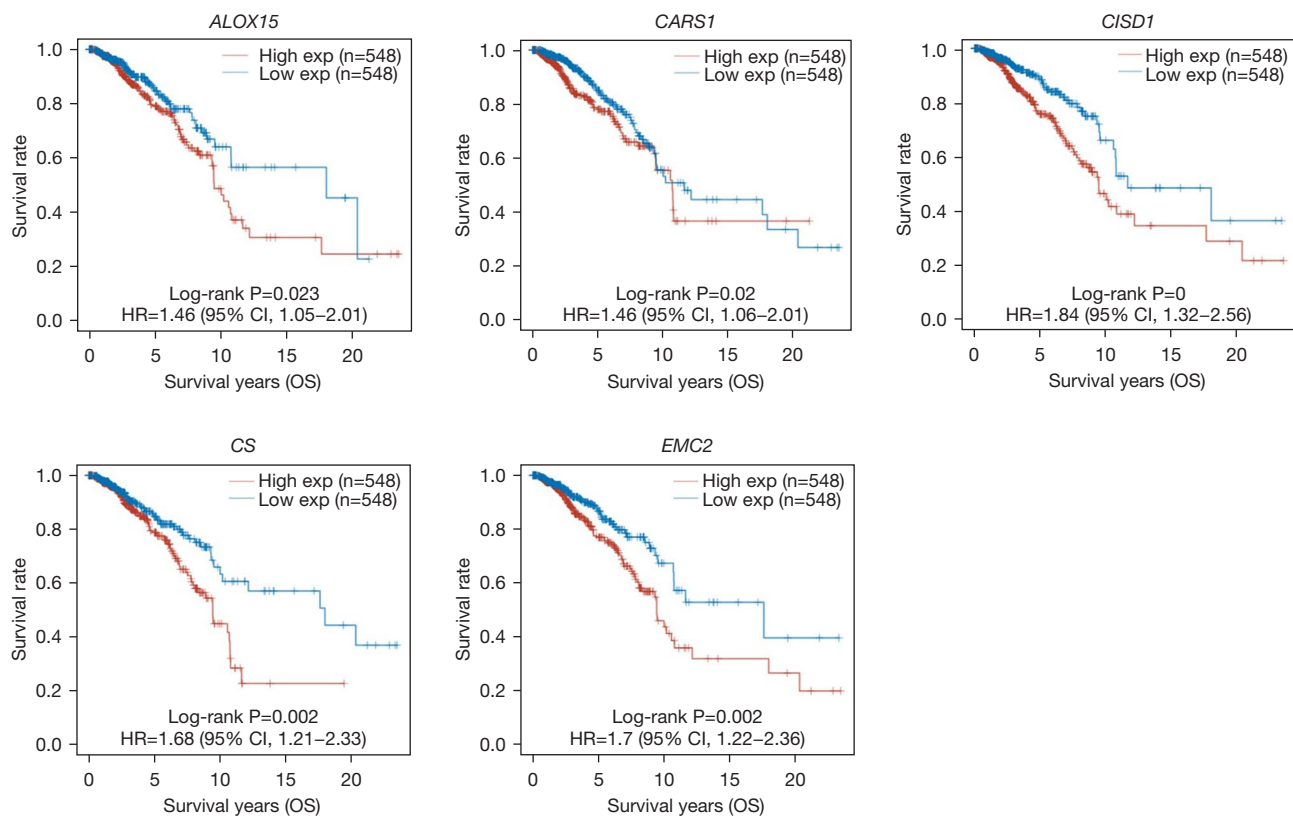


Figure 2 Survival curve of ferroptosis-related genes. Five genes were correlated with survival prognosis in BRCA ($P < 0.05$). High exp, high expression; Low exp, low expression; OS, over survival; BRCA, breast cancer.

BRCA patient nomogram

Univariate and multivariate Cox regression analyses of available clinical indicators, age, pTNM staging, and four ferroptosis-related genes were performed to determine independent prognostic predictors of disease-specific survival. Cox regression analysis showed that after adjusting for confounding factors, pTNM staging and *CISD1*, *ALOX15*, *CARS1*, and *SLC7A11* scores could all be used as independent prognostic factors (Figure 4A,4B). Based on the ferroptosis-related gene risk factors, 3- and 5-year prognostic prediction nomograms of BRCA patients were drawn; the c-index was 0.662 and confidence interval was 0.598–1 (Figure 4C). Evaluation for consistency of the calibration curve showed that the survival rate of the 3- and 5-year prognosis prediction nomogram of patients is in good agreement with the actual survival rate (Figure 4D).

Discussion

As an inevitable biological event in organisms, cell

death plays a vital role in the regulation of homeostasis and development. Ferroptosis, a regulated form of cell death, has different biochemical processes and genetic characteristics mainly driven by iron accumulation, lipid peroxidation, and plasma membrane rupture (13). Compared to normal cells, cancer cells exhibit iron ion aggregation, and regulating ferroptosis from the perspective of iron homeostasis can effectively kill tumor cells (14). In recent years, studies have confirmed that using ferroptosis to induce cancer cell death is effective for advanced tumors and tumor resistance (15,16). In addition to various inducing molecules, many genes can be used as markers of ferroptosis (17). Ferroptosis-related genes have shown good predictive performance in many tumors. BRCA has the highest incidence of malignant tumors in women; however, there are few studies on using ferroptosis-related genes to predict the prognosis of BRCA.

To address this need, we obtained clinical BRCA gene expression data from TCGA database and selected ferroptosis-related genes through a literature search. Here,

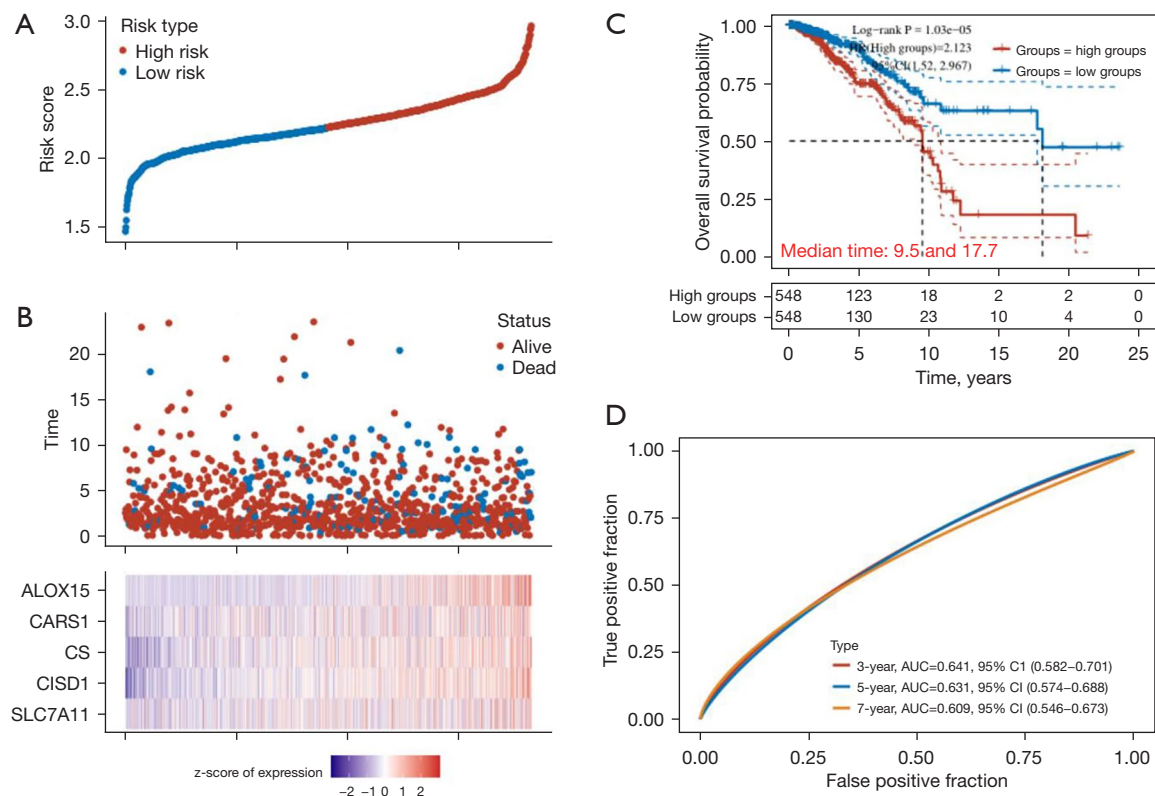


Figure 3 Prognostic models of four ferroptosis-related genes in The Cancer Genome Atlas queue. (A) High and low risk scores in The Cancer Genome Atlas cohort; (B) survival status of patients in the cohort corresponding to five genes; (C) Kaplan-Meier survival curves between high-risk and low-risk groups; (D) receiver operating characteristic curve assessment of the predictive power of 3-, 5-, and 7-year survival. In (A,B) the abscissa of the upper, middle and lower figures represent samples, and the samples are in the same order. AUC, area under the curve.

we analyzed the correlation between ferroptosis-related genes and BRCA through differential gene analysis and determined that 19 ferroptosis-related genes were closely related to BRCA. Survival analysis of these differential genes revealed that four ferroptosis-related genes, *CISD1*, *ALOX15*, *CARS1*, and *SLC7A11*, had significant differences in survival in BRCA. The survival of the high-expression group was significantly lower than that of the low-expression group. LASSO Cox regression analysis was used to construct a prognostic model which divided BRCA patients into high- and low-risk groups. We observed that patients in the low-risk group had longer survival times than those in the high-risk group. In addition, we developed a nomogram, ROC curves, and calibration charts based on the results of the multivariate Cox regression to confirm the predictive ability of the nomogram.

Finally, a risk-scoring model consisting of four ferroptosis-related genes, *CISD1*, *ALOX15*, *CARS1*, and *SLC7A11*, was constructed. As a mitochondrial protein

coding gene, *CISD1* is an important regulator of ferroptosis. Its anti-ferroptosis activity is closely related to changes in the mitochondrial iron accumulation. *CISD1* expression is associated with tumor growth and is a potential therapeutic target (18). *ALOX15* may also be a potential target for cancer treatment, and its expression level can be used as a predictive marker for the clinical outcome of patients with lymph node metastasis and malignant tumors (19). *CARS1* participates in cysteine metabolism and is the rate-limiting agent in glutathione synthesis. Glutathione is an important molecule that can be used as a predictor of ferroptosis in kidney cancer, and it regulates the oxidative environment of cells and ferroptosis (20). *SLC7A11* expression is associated with amino acid transport essential in glutathione homeostasis and protection of cells from oxidative stress; it also plays a key role in oxidative stress signals that are closely related to cell proliferation and tumor growth (21).

In summary, we used bioinformatic analyses to construct a new BRCA prognostic model that contains four

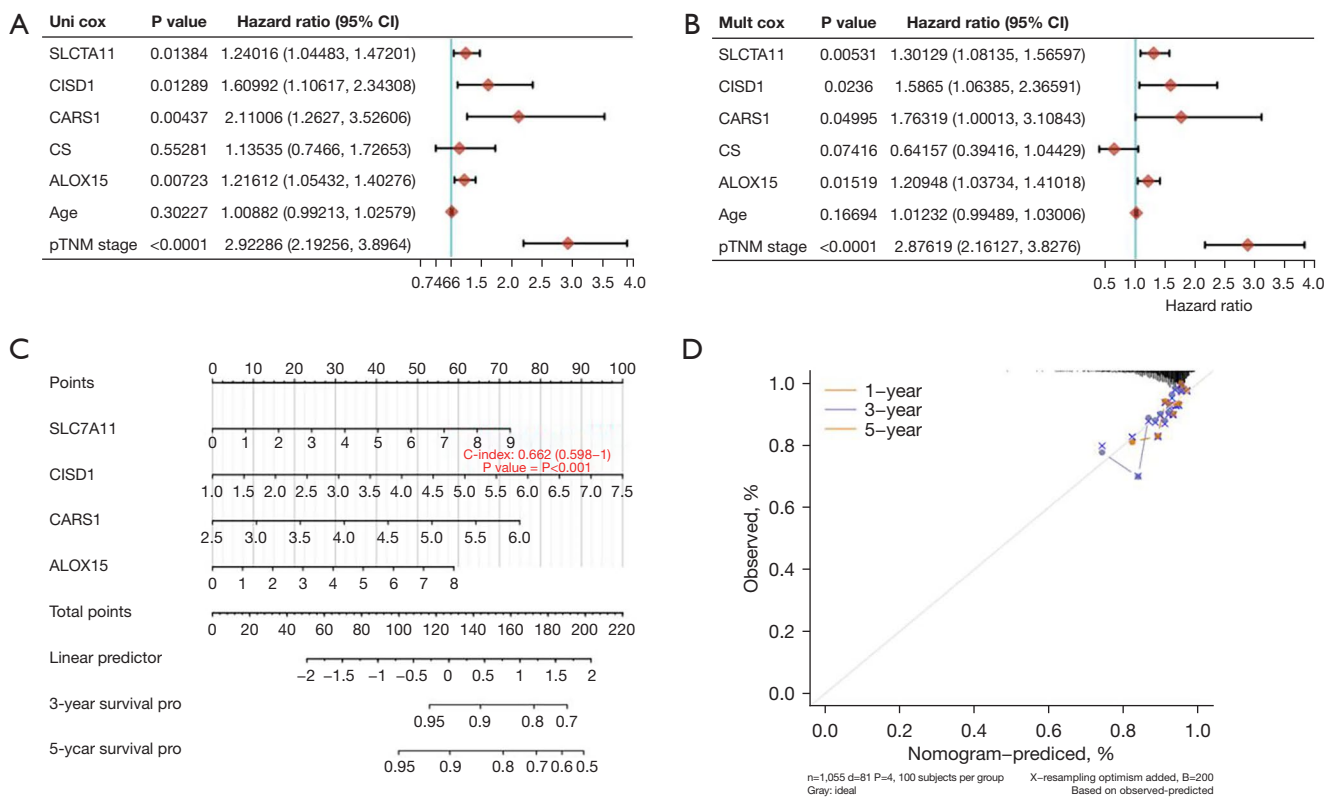


Figure 4 Establishment and accuracy evaluation of the nomogram. (A) Univariate Cox regression analysis; (B) multivariate Cox regression analysis; (C) nomogram of 3- and 5-year disease-specific survival prediction model; (D) disease-specific survival calibration curve. Uni-cox, univariate analysis; Mult-cox, multivariate analysis.

ferroptosis-related genes which can independently predict the overall survival of patients with BRCA. Additionally, a nomogram was developed to accurately predict the prognosis of BRCA. However, there are limitations to the study because the research data came from a database lacking some clinical information. Furthermore, the specific mechanism of the relationship between ferroptosis-related genes and BRCA prognosis needs further study.

Acknowledgments

Funding: This study was supported by Chongqing Science and Health Joint Medical Research Project (No. 2019QNXM027).

Footnote

Reporting Checklist: The authors have completed the STREGA reporting checklist. Available at <https://tcr.amegroups.com/article/view/10.21037/tcr-21-2686/rc>

[amegroups.com/article/view/10.21037/tcr-21-2686/rc](https://tcr.amegroups.com/article/view/10.21037/tcr-21-2686/rc)

Data Sharing Statement: Available at <https://tcr.amegroups.com/article/view/10.21037/tcr-21-2686/dss>

Peer Review File: Available at <https://tcr.amegroups.com/article/view/10.21037/tcr-21-2686/prf>

Conflicts of Interest: All authors have completed the ICMJE uniform disclosure form (available at <https://tcr.amegroups.com/article/view/10.21037/tcr-21-2686/coif>). The authors have no conflicts of interest to declare.

Ethical Statement: The authors are accountable for all aspects of the work in ensuring that questions related to the accuracy or integrity of any part of the work are appropriately investigated and resolved. The study was conducted in accordance with the Declaration of Helsinki (as revised in 2013).

Open Access Statement: This is an Open Access article distributed in accordance with the Creative Commons Attribution-NonCommercial-NoDerivs 4.0 International License (CC BY-NC-ND 4.0), which permits the non-commercial replication and distribution of the article with the strict proviso that no changes or edits are made and the original work is properly cited (including links to both the formal publication through the relevant DOI and the license). See: <https://creativecommons.org/licenses/by-nc-nd/4.0/>.

References

1. Bray F, Ferlay J, Soerjomataram I, et al. Global cancer statistics 2018: GLOBOCAN estimates of incidence and mortality worldwide for 36 cancers in 185 countries. *CA Cancer J Clin* 2018;68:394-424.
2. Li H, Zheng RS, Zhang SW, et al. Incidence and mortality of female breast cancer in China, 2014. *Zhonghua Zhong Liu Za Zhi* 2018;40:166-71.
3. Waks AG, Winer EP. Breast Cancer Treatment: A Review. *JAMA* 2019;321:288-300.
4. Liang Y, Zhang H, Song X, et al. Metastatic heterogeneity of breast cancer: Molecular mechanism and potential therapeutic targets. *Semin Cancer Biol* 2020;60:14-27.
5. Denkert C, von Minckwitz G, Darb-Esfahani S, et al. Tumour-infiltrating lymphocytes and prognosis in different subtypes of breast cancer: a pooled analysis of 3771 patients treated with neoadjuvant therapy. *Lancet Oncol* 2018;19:40-50.
6. Valashedi MR, Najafi-Ghalehlou N, Nikoo A, et al. Cashing in on ferroptosis against tumor cells: Usher in the next chapter. *Life Sci* 2021;285:119958.
7. Jiang M, Qiao M, Zhao C, et al. Targeting ferroptosis for cancer therapy: exploring novel strategies from its mechanisms and role in cancers. *Transl Lung Cancer Res* 2020;9:1569-84.
8. Viswanathan VS, Ryan MJ, Dhruv HD, et al. Dependency of a therapy-resistant state of cancer cells on a lipid peroxidase pathway. *Nature* 2017;547:453-7.
9. Wang W, Green M, Choi JE, et al. CD8+ T cells regulate tumour ferroptosis during cancer immunotherapy. *Nature* 2019;569:270-4.
10. Zheng DW, Lei Q, Zhu JY, et al. Switching Apoptosis to Ferroptosis: Metal-Organic Network for High-Efficiency Anticancer Therapy. *Nano Lett* 2017;17:284-91.
11. Li Z, Chen L, Chen C, et al. Targeting ferroptosis in breast cancer. *Biomark Res* 2020;8:58.
12. Liu Z, Zhao Q, Zuo ZX, et al. Systematic Analysis of the Aberrances and Functional Implications of Ferroptosis in Cancer. *iScience* 2020;23:101302.
13. Liu J, Kuang F, Kroemer G, et al. Autophagy-Dependent Ferroptosis: Machinery and Regulation. *Cell Chem Biol* 2020;27:420-35.
14. Lei P, Ayton S, Bush AI. The essential elements of Alzheimer's disease. *J Biol Chem* 2021;296:100105.
15. Xu G, Wang H, Li X, et al. Recent progress on targeting ferroptosis for cancer therapy. *Biochem Pharmacol* 2021;190:114584.
16. Sui S, Xu S, Pang D. Emerging role of ferroptosis in breast cancer: New dawn for overcoming tumor progression. *Pharmacol Ther* 2022;232:107992.
17. Chen X, Comish PB, Tang D, et al. Characteristics and Biomarkers of Ferroptosis. *Front Cell Dev Biol* 2021;9:637162.
18. Yuan H, Li X, Zhang X, et al. CISD1 inhibits ferroptosis by protection against mitochondrial lipid peroxidation. *Biochem Biophys Res Commun* 2016;478:838-44.
19. Fochtmann-Frana A, Haymerle G, Schachner H, et al. Expression of 15-lipoxygenase-1 in Merkel cell carcinoma is linked to advanced disease. *Clin Otolaryngol* 2018;43:1335-44.
20. Wu G, Wang Q, Xu Y, et al. A new survival model based on ferroptosis-related genes for prognostic prediction in clear cell renal cell carcinoma. *Aging (Albany NY)* 2020;12:14933-48.
21. Ma Z, Zhang H, Lian M, et al. SLC7A11, a component of cysteine/glutamate transporter, is a novel biomarker for the diagnosis and prognosis in laryngeal squamous cell carcinoma. *Oncol Rep* 2017;38:3019-29.

Cite this article as: Wang L, Chen Y, Zhao J, Luo D, Tian W. Analysis and prediction model of ferroptosis related genes in breast cancer. *Transl Cancer Res* 2022;11(7):1970-1976. doi: 10.21037/tcr-21-2686

Table S1 Difference of BRCA ferroptosis-related genes between tumor and normal tissues

Uni_cox	P value	Hazard ratio (95% CI)
DPP4	0.2386	1.08631 (0.94659, 1.24665)
NFE2L2	0.83745	1.03044 (0.77379, 1.37222)
FANCD2	0.13538	1.15497 (0.95596, 1.39539)
TFRC	0.06656	1.1505 (0.99047, 1.3364)
SLC7A11	0.02182	1.16993 (1.02309, 1.33786)
CDKN1A	0.13301	1.13805 (0.96138, 1.34719)
HSPB1	0.72113	1.02214 (0.90633, 1.15274)
FDFT1	0.22853	1.15695 (0.91255, 1.46681)
EMC2	0.00033	1.58055 (1.2309, 2.02951)
RPL8	0.40334	0.91474 (0.7422, 1.12738)
HSPA5	0.55681	1.08697 (0.82302, 1.43558)
NCOA4	0.09801	1.21397 (0.96485, 1.52741)
CISD1	0.001	1.54293 (1.19164, 1.99778)
LPCAT3	0.58466	1.05465 (0.87145, 1.27637)
CS	0.00357	1.60787 (1.16819, 2.21305)
GLS2	0.17325	1.27139 (0.89991, 1.79623)
MT1G	0.68433	1.01537 (0.9434, 1.09282)
GPX4	0.08641	0.81939 (0.65253, 1.02891)
SLC1A5	0.31477	1.1115 (0.90448, 1.36589)
SAT1	0.97104	0.99597 (0.80091, 1.23854)
ATP5MC3	0.02341	1.43425 (1.05, 1.95911)
CARS1	0.01592	1.61478 (1.09373, 2.38408)
ATL1	0.27282	0.90499 (0.75709, 1.08177)
ALOX15	0.00177	1.19034 (1.06715, 1.32776)
ACSL4	0.57768	0.95793 (0.82344, 1.11439)